

# Image Deblurring using a Hybrid Optimization Algorithm

Kit Yan Chan<sup>1</sup>, N. Rajakaruna<sup>2</sup>  
Department of Electrical and Computer Engineering,  
Curtin University, Australia

[kit.chan@curtin.edu.au](mailto:kit.chan@curtin.edu.au)<sup>1</sup>, [Nimali.rajakaruna@curtin.edu.au](mailto:Nimali.rajakaruna@curtin.edu.au)<sup>2</sup>

C. Rathnayake<sup>3</sup>, I. Murray<sup>4</sup>  
Department of Electrical and Computer Engineering,  
Curtin University, Australia

[rchamila@gmail.com](mailto:rchamila@gmail.com)<sup>3</sup>, [i.murray@curtin.edu.au](mailto:i.murray@curtin.edu.au)<sup>4</sup>

**Abstract** — In many applications, such as way finding and navigation, the quality of image sequences are generally poor, as motion blur caused from body movement degrades image quality. It is difficult to remove the blurs without prior information about the camera motion. In this paper, we utilize inertial sensors, including accelerometers and gyroscopes, installed in smartphones, in order to determine geometric data of camera motion during exposure. Based on the geometric data, we derive a blurring function namely point spread function (PSF) which deblur the captured image by reversing motion effect. However, determination of the optimal PSF with respect to the image quality is multi-optimum, as deblurred images are not linearly correlated to image intelligibility. Therefore, this paper proposes a hybrid optimization method, which is, incorporated the mechanisms of particle swarm optimization (PSO) and gradient search method, in order to optimize PSF parameters. It aims to incorporate the advantages of the two methods, where the PSO is effective in localizing the global region and the gradient search method is effective in converging local optimum. Experimental results indicated that deblurring can be successfully performed using the optimal PSF. Also, the performance of proposed method is compared with the commonly used deblurring methods. Better results in term of image quality can be achieved. The resulting deblurring methodology is an important component. It will be used to improve deblurred images to perform edge detection, in order to detect paths, stairs ways, movable and immovable objects for vision-impaired people.

**Index Terms**— image deblurring; inertial sensors; vision impaired navigation; particle swarm optimization; hybrid optimization method

## I. INTRODUCTION

In image acquisition, we aim to capture photos which are used to truly represent the underlying scene that we intend to observe. However, the observation process is never perfect, as image blurriness significantly degrades object structures on the captions and causes poor image quality. Also, the blur can be caused by atmospheric turbulences, incorrect focus settings, camera motion and movement within the scene. For smart phones or tablets, considerable blurs are likely to be generated by body movement when the users are performing navigation. Although fast shutter speeds could reduce the blurs, image noise could be generated. Also, they are usually not available in smart phones or tablets, as camera with these functions are very expensive. Potential dangers for the vision-impaired people can be caused when poor image captions are used for object detection and path identification in the navigation system [1]. To improve the image quality, deblurring algorithm can be applied by removing the

blurred effects. Deblurring methods can be divided into two main types, namely Blind deconvolution and Non-blind deconvolution.

When blurring function namely point-spread function (PSF), is an unknown, the blind deconvolution can be used to improve the quality of blurred images. PSF use the statistical sequences of the blurs in order to remove the blurred patterns. However, the deblurred images are difficult to recover, as camera motions are mostly chaotic and random. Non-blind deconvolution can be used when the PSF is available. Recent technologies of mobile devices enable the estimation of the PSF using the embedded inertial sensors, while the 3-axis accelerometer gives the linear motion and the 3-axis gyroscope gives the angular motion. Geometric data for the camera motion can be used for developing the PSF. However, it is imprecise to use accelerometer signal to compute camera velocity and displacement, as the captured signal is accumulated with noise caused by sensor drift [2], [3]. In addition, an appropriate PSF is difficult to generate for effective deblurring, as the exposure time is relatively short.

In this paper, a deblurring methodology is proposed by using PSF, determined on the geometric information with respect to the three-dimensional linear motion of the camera. The geometric information is used, as most modern smartphones are equipped with three-dimensional accelerometers and gyroscopes, geometric information may be used to measure the linear and rotary motions of the camera. The performance of the PSF is evaluated based on quality of the deblurred image of which an image quality analyzer [19] is used, as the image quality measure is effective to predict the quality of distorted images when a little prior knowledge of the images is available.

However, the relationship between the image quality score and the PSF parameters is not linear, as the deblurred image may not be correlated to the improvement of image intelligibility. The problem on determining the optimal PSF parameters with respect to the image quality score is multi-optimum. Conventional gradient search methods may not be effective to determine the PSF parameters. In this paper, we propose a hybrid optimization method (HOM) which incorporates mechanisms of both local and global search methods. HOM first uses a global optimization method [18], to generate a set of solutions with good image quality scores, as the PSO is effective in performing optimization on multi-optimal problems. After generated the better solution, that result uses a gradient search method to locate the optima with respect to the image quality. The effectiveness of the proposed HOM is evaluated by developing PSF for image deblurring, where the geometric information of the camera motion is captured

by Sony Xperia TX smartphone. Experimental results show that the proposed method can improve the image quality of the deblurred images. Significant improvement can be achieved when the PSF is compared with the commonly used deblurring methods [10] including blind deconvolution, Wiener filter, Lucy-Richardson method and the regularized filter. Additionally the proposed HOM outperforms the other state-of-art heuristic methods including particle swarm optimization, genetic algorithm and simulated annealing.

This paper is organized as follows: Section II discusses previous works related to image deblurring with and without using inertial sensor data. Section III describes the proposed deblurring method in developing the PSF engaged with the inertial sensor data. Section IV presents the proposed HOM in optimizing the PSF parameters. In Section V, experimental results in terms of image quality are presented and also comparison with other methods is given. The conclusion and future work are given in Section VI.

## II. LITERATURE REVIEW AND RESEARCH MOTIVATION

Generally, approaches for image deblurring can be classified into two types, blind deconvolution and non-blind deconvolution [4]. Blind deconvolution is a difficult task, as the PSF is an unknown. Non-blind deconvolution is more effective as the PSF is known. Hence, deblurring regimes can be developed than those when no prior information for the PSF is available. Recent deblurring methods have been developed by incorporating the mechanisms of point spread function (PSF) and non-blind deconvolution.

### A. Blind deconvolution

The common approaches of blind deconvolution are based on the availability of more than two images of the same scene. With a close temporal position, these approaches can be particularly implemented in way finding applications. Rav-Acha and Peleg [5] developed a blind deconvolution using two blurred images with two motion captions of which the correlation between the two captions is used for determining the deblurring function. Lu et al. [6] used a two images of which one is blurry and one is noisy, in order to perform deblurring in low light conditions. However, these approaches cannot be applied on real-time systems such as road navigation or way finding as the required computational time is high.

Fergus et al. [7] developed a method using a single image for handling slight blurring such as camera tremble. It attempts to determine the camera motion based on the initial blur kernel, which is estimated by the heuristic information of camera motion. An additional deblurring method was proposed by Qi et al. [8] based on a unified probabilistic model consisting of both blur kernel estimation and de-blurred image restoration. However, both these methods have complex computational costs and are therefore not suitable for implementing on microcontroller, which has limited computational power.

### B. Non-blind deconvolution

Modern electronic communication devices, such as smart phones and tablets commonly have embedded inertial sensors such as gyroscopes, accelerometers which can be

used to capture inertial data in order to determine the geometric information for the camera motion.

Hyeoung et al. [9] proposed a de-blurring method using the IMU data captured by the gyroscope, accelerometer and depth sensor installed on the camera. The computational cost required for this method is high, as it requires a microcontroller with high computational power to control the position of the depth sensor making it unsuitable for implementation in real-time applications. A more effective deblurring method was developed based on the geometric information captured by accelerometer, gyroscopic sensor data and digital single-lens reflex (DSLR) camera [10-12]. However, this approach requires the expensive DSLR camera and can only be used for offline deblurring.

A deblurring method based on the IMU sensor data has been developed by Sanketi et al. [13]. In this method, both the anti-blur feedback and IMU sensor data are used for the camera stabilization. It is useful in the area of image acquisition but synchronizing the IMU data with the image capture is a challenging task as the accelerometer and the gyroscopic sensor capture IMU data and the camera captures the image within the exposure time. As the exposure time is small, the synchronization task, which attempts to align the image sensor with IMU data, is problematic.

This paper proposes a deblurring methodology, which uses the IMU data, captured by accelerometer and gyroscopic sensor data. A hybrid optimization method has been developed to synchronize the IMU data and the captured image in order to improve the image quality of the blurred images. The resulting deblurring methodology will benefit our research project, which aims to develop an embedded system for way finding purposes for vision-impaired people.

## III. METHODOLOGY

### A. Capturing geometric data for camera motions

Although users attempt to stabilize the camera for general photography, blurred images are occurring. To improve the image quality, deblurring techniques are generally developed to target this kind of motion blur. In the case of way finding applications, body movements of users blur the images and thus controlling the movements of cameras is not a realistic proposition. Hence, identifying the geometrical information of the camera motions is a key in order to develop computational algorithms for deblurring purposes. The accelerometers and the gyroscopes are generally used to estimate the geometric information of camera motions, as most of high-end smartphones are equipped with a three-dimensional accelerometer and a three-dimensional gyroscope that can be used to measure the linear and rotary motions of the camera installed on the smartphone.

However, the issues in using the accelerometer to compute the linear displacement are the gravity component present in accelerometer data [2], the drift caused by the double integral [3] and the fact that the initial velocity is unknown. Further drift is occurred when the angular displacement is computed [3].

As the blurriness of an image is usually caused by linear and angular movements of the camera, the scene captured by the camera can be considered as moving with respect to the camera if we assume that the camera is stationary. Hence, the PSF, which illustrates the relative motion of the scene, are caused by the linear and rotary movements of the camera. As the zooming effect is caused by the perpendicular component, a linear blur is generated by the component on the scene plane.

Figure 1 shows the scene plane with respect to the camera, where the distance between the scene plane and the camera is defined as  $l$ . At time  $t$ , the velocity components of the point  $(a, b)$  are shown in the figure, where  $A_x(t)$ ,  $A_y(t)$  and  $A_z(t)$  represent the linear acceleration of camera along  $x$ ,  $y$  and  $z$  axis respectively;  $V_x(t)$ ,  $V_y(t)$  and  $V_z(t)$  represent the linear velocity of camera along  $x$ ,  $y$  and  $z$  axis respectively;  $\omega_x(t)$ ,  $\omega_y(t)$  and  $\omega_z(t)$  represent the angular velocity of camera along  $x$ ,  $y$  and  $z$  axis; and  $v_x(t)$ ,  $v_y(t)$  and  $v_z(t)$  represents linear velocity of frame with respect to camera along  $x$ ,  $y$  and  $z$  axis.

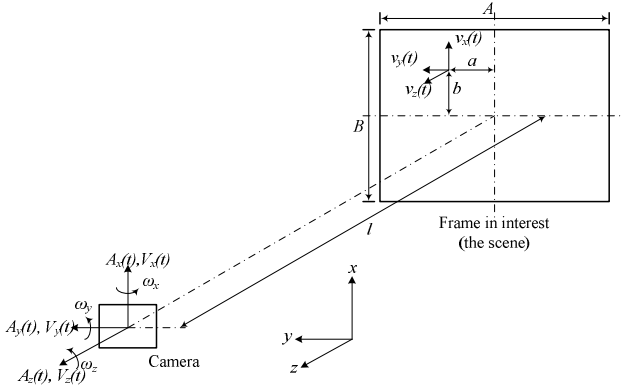


Figure 1 Illustration of the scene with respect to the camera

$v_x(t)$ ,  $v_y(t)$  and  $v_z(t)$  can be computed based on equations (1), (2) and (3) respectively.

$$v_x(t) = -V_x(t) + l\omega_y(t) + a\omega_z(t), \quad (1)$$

$$v_y(t) = -V_y(t) - l\omega_x(t) - b\omega_z(t), \quad (2)$$

$$v_z(t) = -V_z(t) - a\omega_x(t) + b\omega_y(t). \quad (3)$$

The contribution of linear velocity components,  $V_x(t)$ ,  $V_y(t)$  and  $V_z(t)$ , to the velocity of the point on the scene is very small compared to the contribution from angular velocity,  $\omega_x$ ,  $\omega_y$  and  $\omega_z$ . Hence,  $V_x(t)$ ,  $V_y(t)$  and  $V_z(t)$ , can be omitted from (1), (2) and (3) and the following formulations can be used to compute the velocity of the point on the scene.

$$v_x(t) = l \cdot \omega_y(t) + a \cdot \omega_z(t), \quad (4)$$

$$v_y(t) = -l \cdot \omega_x(t) - b \cdot \omega_z(t), \quad (5)$$

$$v_z(t) = -a \cdot \omega_x(t) + b \cdot \omega_y(t). \quad (6)$$

After  $v_x(t)$ ,  $v_y(t)$  and  $v_z(t)$  are computed, the linear displacements,  $D_x(t)$ ,  $D_y(t)$  and  $D_z(t)$ , with respect to  $x$ ,  $y$  and  $z$  can be computed respectively by iterating each linear velocity component using trapezoid rule as

$$D_x(t) = D_x(t-T) + (v_x(t) - v_x(t-1)) \cdot T, \quad (7)$$

$$D_y(t) = D_y(t-T) + (v_y(t) - v_y(t-1)) \cdot T, \quad (8)$$

$$D_z(t) = D_z(t-T) + (v_z(t) - v_z(t-1)) \cdot T, \quad (9)$$

where  $T$  is the sampling period.

### B. Determination of the PSF matrix

Although linear displacements can be captured for the camera motions, the PSF against camera motions cannot be determined precisely as both the parameters of camera size and the focal length are usually an unknown. Both parameters are not usually provided by the vendors. In order to improve the precision, an empirical measurement was taken to find the ratio  $B/l$ , and  $B/A = 3/4$  was used during this measurement. The dimensions of the frame with respect to  $A$  and  $B$  were computed using the ratio of  $B/l$  measured. If the resolution of the image is given as  $m \times n$  with the ratio of  $m:n = 4:3$ , the number of pixels at the scene can be computed as  $A/m$  or  $B/n$ . Based on this resolution information, the total pixel displacements with respect to  $x$  and  $y$  axis can be computed and they are the dimensions of PSF matrix.

The next task was to compute the parameters of the PSF matrix based on the computed displacements. As some of the pixel points between the two consecutive sample points (i.e.  $(D_x(t), D_y(t))$  and  $(D_x(t+T), D_y(t+T))$ ) are empty in the image, linear interpolation was used to fill the gap between those empty samples. Figure 2 shows the algorithm which is used to derive the PSF from computed displacements on the plane of the scene. The movement along  $z$ -axis was not incorporated in this computation so that the zooming function of the camera can be considered separately.

```

Set (Total number of sampling points)  $\rightarrow N$ 
Set  $(D_x(N \cdot T) - D_x(0)) \rightarrow x\_span$  ;
Set  $(D_y(N \cdot T) - D_y(0)) \rightarrow y\_span$  ; Set  $0 \rightarrow c$ 
for  $i = 1$  to  $N$  do
  if  $(x\_span > y\_span)$ 
    Set  $N_f$  be the number of fill up pixels between
       $D_x(i \cdot T)$  and  $D_x((i+1) \cdot T)$  .
  else
    Set  $N_f$  be the number of fill up pixels between
       $D_y(i \cdot T)$  and  $D_y((i+1) \cdot T)$  . endif
  Create the coordinates,  $(X(j), Y(j))$ , based on the
    interpolation between  $(D_x(i \cdot T), D_y(i \cdot T))$  and
       $(D_x((i+1) \cdot T), D_y((i+1) \cdot T))$ , where
       $j = (c+1), (c+2), \dots, (N_f + c)$  .
  Set  $(c+1+N_f) \rightarrow c$ 
for  $j = 0$  to  $c$  do
   $col = \text{Round}(Y(j))$ 
   $row = \text{Round}(X(j))$ 
   $\text{PSF}(col, row) = \text{PSF}(col, row) + 1$ ; endfor
endfor

```

Figure 2 Algorithm for determining the PSF matrix

As the parameters of the PSF matrix are dependent on the relative motion,  $D_x(t)$  and  $D_y(t)$ , which can be adjusted by the alignment parameters,  $a$ ,  $b$  and  $l$ , formulated in equations (7), (8) and (9). An effective PSF can only be developed when the optimal alignment parameters are

used. In the following section, a hybrid optimization method (HOM) incorporated with particle swarm optimization algorithm (PSO) [18] and gradient search method is proposed in order to determine the optimal alignment parameters. Deblurred image with optimal image quality can generated, when the PSF engaged with the optimal alignment parameters are used.

#### IV. HOM FOR OPTIMIZING PSF MATRIX

Although the gradient search method can be used to determine the optima of the PSF by systematically moving the solution space, there is no guarantee that the global optimum of the PSF can be searched due to the nonlinearity of the camera motion and the image quality measure [19]. Another commonly used heuristic method, PSO, has been demonstrated on solving many hard optimization problems, but PSO would take relatively longer convergence time to converge than the gradient search method.

In this research, the HOM which is incorporated with PSO and gradient search method is proposed in order to seek the optimal PSF. The best particle obtained by the PSO is used as the initial solution of the gradient search method. Hence, the global optimum of the PSF can be seek more effectively by the gradient search method than solely using the PSO.

First, the HOM generate  $N_s$  particles randomly, where the position of the  $j$ -th particle at the  $g$ -th generation is represented by:

$$P_j^g = (\kappa_{j,1}^g, \kappa_{j,2}^g, \kappa_{j,3}^g); \quad (10)$$

$g=1$ ;  $\kappa_{j,1}^g$ ,  $\kappa_{j,2}^g$ ,  $\kappa_{j,3}^g$  are represented by three alignment parameters namely  $a$ ,  $b$  and  $l$  respectively; all  $\kappa_{j,k}^g$ , with  $k=1, 2, 3$ , are generated randomly within their operational ranges, given as  $\kappa_{j,1}^g \in [a_{\min} \cdot a_{\max}]$ ,  $\kappa_{j,2}^g \in [b_{\min} \cdot b_{\max}]$  and  $\kappa_{j,3}^g \in [l_{\min} \cdot l_{\max}]$ .

All  $\kappa_{j,k}^g$ , with  $k=1, 2, 3$ , are evaluated based on quality of the deblurring image which are determined using the image quality analyzer [19]. When  $g>1$ , each  $P_j^g$  are updated by the following formulation:

$$\kappa_{j,k}^g = \kappa_{j,k}^{g-1} + vel_{j,k}^g, \quad (11)$$

where  $vel_{j,k}^g$  is the velocity of  $\kappa_{j,k}^g$  which is given by,

$$vel_{j,k}^g = C \left( v_{j,k}^{g-1} + \phi_1 \cdot \gamma \cdot (pbest_{j,k} - \kappa_{j,k}^{g-1}) + \phi_2 \cdot \gamma \cdot (gbest_k - \kappa_{j,k}^{g-1}) \right) \quad (12)$$

$$pbest_j = [pbest_{j,1}, pbest_{j,2}, pbest_{j,3}], \text{ and}$$

$$gbest = [gbest_1, gbest_2, gbest_3];$$

$pbest_j$  denotes the best previous position of a particle recorded from the previous generation;  $gbest$  denotes the position of the best particle among all particles;  $\gamma$  denotes a random number in the range of  $[0,1]$ ;  $w$  is an inertia weight factor;  $\phi_1$  and  $\phi_2$  are the acceleration constants

[1]; and  $C$  denotes the constriction factor, that ensures the PSO converges [2], which is given by:

$$C = \frac{2}{\left| 2 - \phi - \sqrt{\phi^2 - 4\phi} \right|}, \text{ with } \phi = \phi_1 + \phi_2 \text{ and } \phi > 4. \quad (13)$$

The PSO utilizes  $pbest_j$  and  $gbest$  to modify the current location of all  $\kappa_{j,k}^g$  in order to prevent them from moving in the same direction, but to converge gradually towards  $pbest_i$  and  $gbest$  [3]. To further refine the dynamic of  $\kappa_{j,k}^g$ ,  $vel_{j,k}^g$  is limited by a value which was set as 10%–20% of its range. This limit is employed to avoid  $\kappa_{j,k}^g$  ( $\sigma_i$ ) from flying past good solutions or exploring insufficient local solutions.

In the beginning of the search, the HOM attempts to spread the particles to obtain the appropriate PSF parameters. After several iterations, the searching progress becomes slow. The particle search is terminated when the searching progress converges, then the gradient search method is used to search the optimal PSF parameters as it is more effective to locate the local optimum than the PSO. The best particle generated by the PSO given by equation (14) is used as the initial solution of the gradient search method. It speeds up the process on obtaining the optimal PSF parameters.

$$\bar{\kappa}^{best} = [\kappa_{j,1}^{best}, \kappa_{j,2}^{best}, \kappa_{j,3}^{best}] \quad (14)$$

The pseudo code of the HOM is given as following:

- Step 1:** Generate  $P_j^g$  randomly with  $j = 1, 2, \dots, N_s$  and  $g = 0$ .
- Step 2:** Evaluate  $P_j^g$  based on the image quality analyzer discussed in [19].
- Step 3:** Set  $t=t+1$ .
- Step 4:** Update the velocities  $vel_{j,k}^g$  with  $j=1, 2, \dots, N_s$  and  $k=1, 2, 3$  based on equation (12).
- Step 5:** Generate the particles  $\kappa_{j,k}^g$  based on (11).
- Step 6:** Evaluate the image quality of the PSF represented by each particle  $\kappa_{j,k}^g$  based on the image quality analyzer discussed in [19].
- Step 7:** Goto Step 3, if the termination condition is not reached. Otherwise Goto Step 8.
- Step 8:** Select the best particle,  $\bar{\kappa}^{best}$  in equation (14), among all particle.
- Step 9:** Use gradient search method to determine the optimal PSF parameters using  $\bar{\kappa}^{best}$  as the initial solution.

#### V. RESULTS AND ANALYSIS

This experiment was carried out using a Sony Xperia TX smartphone. The images and geometrical data were captured by the camera and the synchronized inertial sensor respectively, while the camera motions simulate the movement when people are doing navigation. It has been indicated by the captures that, for a time period of 200 ms, the drift caused by the accelerometer integration is in the range of 0.1 mm. This time period was used, as

the exposure time of capturing an image is generally under 100 ms [15].

Figure 2 shows the linear and angular displacements captured by the accelerometer and gyroscope sensor, during image capture. Figure 3 depicts the original image captured by the camera, where the blurring effect can clearly be observed.

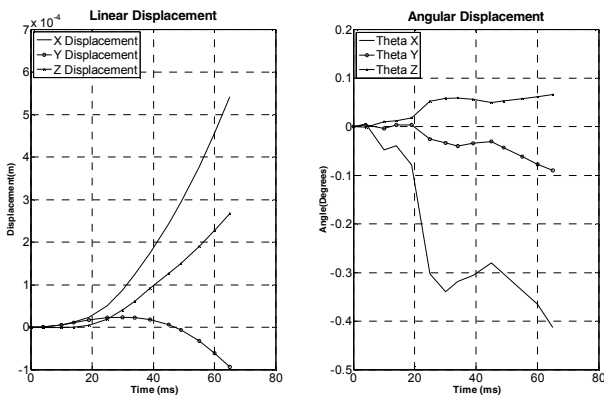


Figure 2: Linear and angular displacements caused by the camera motions with respect to the scene



Figure 3: Original image captured by the camera



Figure 4: Deblurred image generated by the Filter-(HOM)

The five commonly used deblurring methods [10] namely Blind Deconvolution, Wiener filter, Lucy-Richardson method, and regularized filter, were used to deblur the original image. The computed PSF was used in the deblurring methods except the blind deconvolution method, as PSF is not required in the blind deconvolution method. The alignment parameters (i.e.  $a=4$ ,  $b=3$  and  $l=2$ ) defaulted by the camera manufacturer were used on the PSF. Apart from using the default alignment parameters, the proposed method (HOM), genetic algorithm (GA) [20], simulated annealing (SA) [21] and particle swarm optimization (PSO) algorithm [18] have been used to find

the optimal alignment parameters for developing the PSF. For these four methods, the regularized filter was used as the deblurrer and the alignment parameters searched by the four methods was used to develop the PSF. Here the PSF optimized by the GA, SA, PSO and HOM are denoted as Filter-(GA), Filter-(SA), Filter-(PSO) and Filter-(HOM) respectively. The number of particles (or chromosomes) used on Filter-(GA), Filter-(PSO) and Filter-(HOM) are 20. The number of iterations used on Filter-(PSO) and Filter-(GA) are 50. The number of evaluations performed on Filter-(SA) is same as those used in Filter-(PSO) and Filter-(GA) which is 1000. The number of evaluations used on Filter-(HOM) is variable, as the search

of the Filter-(HOM) is terminated when it is converged to a solution. As Filter-(GA), Filter-(HOM) and Filter-(PSO) are heuristic methods, different results can be obtained with different runs. Hence, each method was run for 30 times, and the average results were recorded.

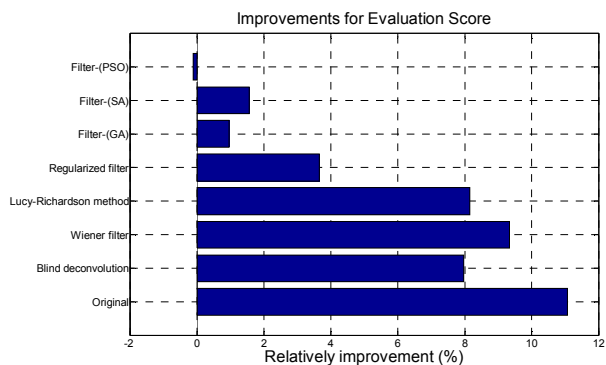
Figure 4 shows that the deblurred image which is processed by the PSF determined by the proposed method (HOM). Although it clearly shows that the deblurred image is superior than the original blurred image, it is difficult to evaluate the image quality by observing solely the deblurred images. To improve the objectivity of the image quality measure, a technique developed by Mittal et al. [19] is used to evaluate the deblurred image. In this method, the image quality measure is effective in predicting the quality of distorted images with little prior knowledge of the images or their distortions. Table I shows that the evaluation scores obtained by different methods, where a smaller evaluation score indicates that the image has a better perceptual quality. It shows that the original image is the poorest, which is also poorer than all those deblurring images. The evaluation scores obtained by the blind deconvolution method, wiener filter and Lucy-Richardson method are poorer than those obtained by the Filter-(GA), Filter-(SA), Filter-(PSO) and Filter-(HOM).

Table I: Image quality evaluation for the tested methods

Deblurring Methods	Evaluation Score	Relative improvement (Percentage)
Original image	19.87	11.072
Blind deconvolution	19.20	7.9687
Wiener filter	19.49	9.3381
Lucy-Richardson method	19.24	8.1601
Regularized filter	18.34	3.6532
Filter-(GA)	17.84	0.95291
Filter-(SA)	17.95	1.5599
Filter-(PSO)	17.65	-0.11331
Filter-(HOM)	17.67	Nil

To further illustrate the performance of the proposed Filter-(HOM), Table I identifies the relative improvements when each of the tested methods is compared with the proposed method, where the improvement is relevant to the exact difference between the proposed Filter-(HOM) to the other tested method. To illustrate more clearly, the relative improvements are shown in Figure 5. For the evaluation scores, the proposed

Filter-(HOM) obtained improvements with more than 10% relative to Blind Deconvolution, Wiener filter, and Lucy-Richardson method. Similar results can be achieved when compared with Filter-(GA), Filter-(SA) and Filter-(PSO) for which optimization of PSF was involved. Also, the proposed Filter-(HOM) obtained an improvement with more than 3.5% relative to the regularized filter.



**Figure 5:** Improvement for evaluation scores achieved by the proposed Filter-(HOM) compared with the other tested method

To further illustrate the effectiveness of the proposed Filter-(HOM), the relative improvements in term of the computational time are shown in Figure 6. They indicate the relative differences between the computational time spent on the proposed Filter-(HOM) and the other tested methods. The figure shows that the relative improvements with 74% can be achieved by the proposed method, compared with the other tested optimization methods. This improvement regarding computational time further indicates the effectiveness of the proposed method, Filter-(HOM).

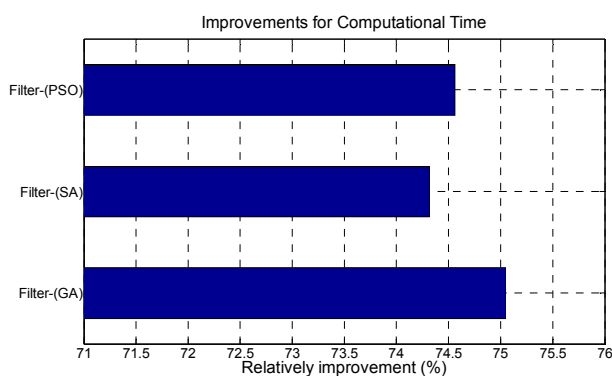


**Figure 6:** Improvement for computational time achieved by the proposed Filter-(HOM) compared with the other tested optimization methods

## VI. CONCLUSION AND FUTURE WORK

In this paper, a hybrid optimization method is proposed to determine the optimal PSF using geometric data captured from inertial sensors of smartphones, in order to improve the image quality of the captured image. This hybrid optimization method incorporates the advantages of the PSO and the gradient search method, where the PSO is effective in localizing the global region and the gradient search method is effective in converging local optimum. Experimental results show that the proposed method can improve the image quality of the deblurred images. Significant improvement can be achieved when comparing with the commonly used deblurring filters

including blind deconvolution, Wiener filter, Lucy-Richardson method and the regularized filter. Also, the PSF obtained by the proposed method outperforms those obtained by the state-of-art heuristic methods including PSO, GA and SA.

In the future, the two research directions will be focused. a) In this paper, the hybrid optimization method is only developed by incorporating with two state-of-art methods namely particle swarm optimization and gradient method. Incorporation of PSO with other intelligence methods such as fuzzy system [22], genetic programming [23,24], and neural networks [25] will be studied in order to further improve the searching effectiveness. b) One of the limitations of the proposed method is the accuracy of the accelerometer and the distortion caused by deblurring which can generate ringing artifacts. We will reformulate the optimization problem in order to maximize the image quality and minimize the image distortion. Better PSF is expected to be generated.

## REFERENCES

- [1] N. Rajakaruna and I. Murray, "Edge detection for Local Navigation System for Vision Impaired People Using Mobile Devices", International Conference on Mathematical Sciences & Computer Engineering, Malaysia, pp. 29-30, 2012.
- [2] K. Abhayasinghe and I. Murray, "A novel approach for indoor localization using human gait analysis with gyroscopic data," Third International Conference on Indoor Positioning and Indoor Navigation, 2012.
- [3] D. Sachs. Google Tech Talk, Topic: "Sensor Fusion on Android Devices: A Revolution in Motion Processing." [On-Line], Aug. 2, 2010.
- [4] D. Kundur and D. Hatzinakos, "Blind image deconvolution", IEEE Signal Processing Magazine, IEEE, vol.13, no.3, pp.43-64, 1996.
- [5] A. Rav-Acha and S. Peleg, "Two motion blurred images are better than one", Pattern Recognition Letters, vol 26, pp. 311-317, 2005.
- [6] L. Yuan, J. Sun, L. Quan, and H.Y. Shum, "Image deblurring with blurred/noisy image pairs", ACM SIGGRAPH, 2007.
- [7] R. Fergus, B. Singh, A. Hertzmann, T. Sam and T. William, "Removing camera shake from a single photograph", ACM SIGGRAPH, 2006.
- [8] Q. Shan, J. Jia and A. Agarwala, "High-quality motion deblurring from a single image", ACM SIGGRAPH, 2008.
- [9] B. Hyeoungcho, C.C. Fowlkes, and P.H. Chou, "Accurate motion deblurring using camera motion tracking and scene depth", IEEE Workshop on Applications of Computer Vision, pp. 15-17, 2013
- [10] R. Horstmeyer, "Camera Motion Tracking for De-blurring and Identification", MIT Media Lab MAS 863 Final Project 2010.
- [11] J. Feng, L. Tian, "Digital image stabilization system based on inertial measurement module", School of Automation, Beijing Institute of Technology, China, 2013.
- [12] N. Joshi, S.B. Kang, and C.L. Zitnick, and R. "Szeliski, Image deblurring using inertial measurement sensors", ACM SIGGRAPH, 2010.
- [13] P.R. Sanketi and J.M. Coughlan, "Anti-blur feedback for visually impaired users of smartphone cameras", ACM SIGACCESS, 2010.
- [14] O. Šindelář and F. Šroubek F, "Image deblurring in smartphone devices using built-in inertial measurement sensors", Journal of Electronic Imaging, 2013.
- [15] A. Davis, "What are the shutter speed and ISO ranges for the iPhone 4S camera?" [Weblog entry]. Ask Different, 2012. Available: <http://apple.stackexchange.com/questions/49556/what-a-re-shutter-speed-and-iso-ranges-for-the-iphone-4s-camera>
- [16] R.C. Eberhart and Y. Shi, "Comparison between genetic algorithms and particle swarm optimization", in Evolutionary Programming VII. New York: Springer-Verlag, LNCS, vol. 1447, pp. 611-616, 1998.
- [17] F. Bergh and A.P. Engelbrecht, "A study of particle swarm optimization particle trajectories", Information Sciences, vol. 176, no. 8, pp.937-971, 2006.
- [18] K.E. Parsopoulos and M.N. Vrahatis, "On the computation of all global minimizers through particle swarm optimization", IEEE Transactions on Evolutionary Computation, vol. 8, no. 3, pp. 211-224, 2004.

- [19] A. Mittal, R. Soundararajan, and A.C. Bovik, "Making a Completely Blind Image Quality Analyzer", *IEEE Signal Processing Letter*, vol. 20, pp. 209-212, 2013.
- [20] D.E. Goldberg, *Genetic Algorithms in Search, "Optimization and Machine Learning"*, Addison Wesley Longman Publishing Co., Inc. Boston, MA, USA, 1989.
- [21] S. Kirkpatrick, C.D. Gelatt, and M.P. Vecchi, "Optimization by Simulated Annealing", *Science*, vol. 220, pp. 671-680, 1983.
- [22] C.K. Kwong, K.Y. Chan, H. Wong, Takagi-Sugeno neural fuzzy modeling approach to fluid dispensing for electronic packaging, *Expert Systems with Applications*, vol. 34, no. 3, pp. 2111-2119, 2008.
- [23] K.Y. Chan, C.K. Kwong, T.S. Dillon, Y.C. Tsim, Reducing overfitting in manufacturing process modeling using a backward elimination based genetic programming, *Applied Soft Computing*, vol. 11, no. 2, pp. 1648-1656, 2011.
- [24] K.Y. Chan, C.K. Kwong, T.C. Wong, Modelling customer satisfaction for product development using genetic programming, *Journal of Engineering Design*, vol. 22, no. 1, pp. 55-68, 2011.
- [25] K.Y. Chan, T.S. Dillon, J. Singh, E. Chang, Neural-network-based models for short-term traffic flow forecasting using a hybrid exponential smoothing and Levenberg-Marquardt algorithm, *IEEE Transactions on*, vol. 13, no. 2, pp. 644-654, pp. 2012.